

# Characterization of flood plain and climate change using multi-proxy records from the Mahi River Basin, Mainland Gujarat

**D.A.Sant, K.Krishnan<sup>1</sup>, G. Rangarajan<sup>2</sup>, N.Basavaiah<sup>3</sup>, C.Pandya, M.Sharma and Y.Trivedi**

Department of Geology, M. S. University of Baroda, Vadodara- 390 002

<sup>1</sup>Department of Archaeology and Ancient History, M. S. University of Baroda, Vadodara- 390 002

<sup>2</sup>Centre for Theoretical Studies and the Department of Mathematics, Indian Institute of Science, Bangalore- 560 012

<sup>3</sup> Indian Institute of Geomagnetism, Kalamboli, New Panvel, Navi Mumbai- 410 218

(Email: dasant-geology@mail.msubaroda.ac.in or dhananjay\_sant@yahoo.com)

## ABSTRACT

Sedimentary succession at Bhimpura from the lower reaches of Mahi flood plain (situated in western India) is characterized using parameters such as grain size, magnetic susceptibility, carbonates, ferri-magnetic and other rock forming and clay mineral concentrations. Of the 1513 cm sediment record, the interval spanning 0-580 cm is analyzed and compared with the sediment character of the well-dated section at Rayka. The interpolated age model suggests that the sediments under study fall within the time span of 30 ka to 10 ka. This study has identified strong and weak monsoon events, represented as fluvial/ aeolian sediment characters within the massive unstratified sandy-silty sediment of the Mahi flood plain. Since these sediments form a blanket cover over western India, the response to regional and global climate change is discussed.

## INTRODUCTION

The flood plain sediments preserve history of climatic changes (Knox 2000; Castelltort & Driessche 2003). The reconstruction of flood plain history employs a large variety of methods. These methods essentially lead to the characterization of sediments, which is useful for reconstructing environmental conditions. The properties, which show close relation with the environmental parameters, are called "proxies". These proxies may be defined as measurable descriptors for desired, but unobservable variables. Allogenic character is probably the most important parameter for describing the conditions of continental processes (intensity and type: fluvial/aeolian process) and is crucial for climate modeling (Xiao et al. 1995; Knox 2000; Castelltort & Driessche 2003 and references cited therein). Besides, the authigenic characters are also taken into account to explain in-situ, post-depositional processes. Proxies investigated in the present study for allogenic and authigenic properties are: 14 grain size fractions, sediment facies, ferrimagnetic percentage, magnetic susceptibility, carbonate percentage, calcrete percentage, and mineralogy of the sediment.

The sediment characteristics are important in modelling the continental processes, which otherwise is much more difficult to reconstruct. Lake sediments

are commonly used to decode changes over the continent. Flood plains, on the other hand, have enough potential as they capture climatic signatures and are also widespread, thereby playing a crucial role in the development of the continental landscape (Macklin & Lewin 2003).

In the case of monsoonal rivers, where rainfall is seasonal and region is tectonically stable, the drainage basin response is largely due to a single variable - 'climate'. Characterization of flood plain sediment would therefore capture changes in the processes influenced by regional variation in monsoonal precipitation. This in turn is controlled by large-scale climate dynamics - the Southwest Indian Monsoon (SwIM). Large areas of the world's largest continents, such as Asia and Africa, are influenced by SwIM system, which ultimately forms the backbone for the economy of the countries in these regions.

So far fewer studies have been carried out to observe temporal changes in sediment/environment characteristics found in flood plains either spatially or from a single site from continental landforms. The massive unstratified sandy-silty sediment from flood plain remains unexplored. This study investigates temporal changes in grain size spectra by examining stratigraphy using a range of physical and statistical parameters for the massive unstratified sandy-silty sediment of Mahi flood plains. At the same time

efforts are made to characterize stronger and weaker phases of monsoon. Also, various global climatic stages and its response along western India are investigated regarding the final stages of Last Glacial phase.

This study deals with multi-proxy data that was generated for the first time from Bhimpura [22°19'08.58"N, 73°05'00.97"E, 33.3m a.s.l] situated in the southern Cambay alluvial plain of tropical India (Fig. 1). Cambay alluvial plain (CAP) forms a vast stretch of flat land having mean elevation of 40m a.s.l, defined over the Cambay rift zone between Saurashtra and Aravalli uplands. Towards the north, the CAP merges with Indus plain and towards the south the plain merges with Gulf of Cambay that opens into Arabian Sea. The present site lies along the southwest Indian monsoon track (Shukla 1975; Shukla & Mishra 1977). Geomorphologically, Bhimpura site falls along the southeastern edge of Mahi flood plain that flows into the Gulf of Cambay. The rationale for selecting the site away from the active channel/ central part of flood basin is that the edge of the flood basin can better capture both major and minor events that occurred in the basin. Sediment deposited at such a site is likely to have appropriate thickness representing both major and minor events. Otherwise, a large amount of sediment from a single event could mask the signature of other events.



**Figure 1.** Location map for the area under study.

Previous works undertaken in the region of Mahi and Sabarmati have led to significant progress in understanding various features of Quaternary sediments. These include studies pertaining to stratigraphy and environment of deposition (Pant & Chamyal 1990; Merh & Chamyal 1997; Tandon et al. 1997; Malik et al. 1999), paleoclimatic reconstructions (Wasson et al. 1983; Sridhar et al. 1994; Tandon et al. 1997; Tandon 1998; Khadkikar et al. 1999; Juyal et al. 2000; Srivastava et al. 2001), role of man in the region (Zeuner 1950; Subbarao 1952; Allchin & Goudie 1971; Goudie & Hegde 1978), and chronology using thermoluminescence method (Tandon et al. 1997; Juyal et al. 2000; Srivastava et al. 2001; Juyal et al. 2003). In addition to this, various earlier workers have also compared fluvial sequence (sedimentology) within and across Mahi and Sabarmati flood basins (Khadkikar et al. 1999; Juyal et al. 2000; Srivastava et al. 2001). Recently, Juyal et al. (2003) have explained aeolian sediments and respective climatic events by studying dunes from mainland Gujarat, south of Thar desert.

## METHODOLOGY

A fifteen-meter open step trench was cut in 14 benches. Each bench was scraped, cleaned and studied for sedimentary structures, nature of pedogenesis and other field evidences. Samples were collected at about 15 cm interval such that all lithological changes have been represented. A total number of 102 samples were collected from 1513 cm section, of which the interval spanning 0-580 cm has been investigated. The samples were subjected to grain-size analysis, magnetic susceptibility, ferrimagnetic mineral percentage, mineralogy and carbonate percentage.

Grain-size analysis was performed by taking 100gm of sample (sample for analysis was taken using conning-quartering method) using dry sieve method. For grain size characterization, fourteen sieve fractions are taken, namely, 420  $\mu$ m, 250  $\mu$ m, 210  $\mu$ m, 149  $\mu$ m, 125  $\mu$ m, 106  $\mu$ m, 90  $\mu$ m, 75  $\mu$ m, 63  $\mu$ m, 53  $\mu$ m, 45  $\mu$ m, 37  $\mu$ m, 25  $\mu$ m and <25  $\mu$ m. Magnetic susceptibility analysis was performed on bulk samples using Bartington MS2 magnetic susceptibility meter operating at two frequencies (0.47kHz and 4.7kHz) for measurement of low frequency mass susceptibility ( $\chi_{LF}$ bulk) and frequency dependent magnetic susceptibility ( $\chi_{FD}$ [%]bulk). Carbonate percentages were calculated on <25  $\mu$ m using standard 1N HCL treatment method. Magnetic mineral percentages were calculated after separation of magnetic minerals using hand magnet from 10gm of bulk sample for all the samples. The mineralogy (7 proxies: quartz, feldspars,

calcites, smectite, chlorite, illite, and hematite) was done using XRD, Philips PW1840 on  $<25\mu\text{m}$  fraction at 45 cm interval (source Cu K $\alpha$  source ( $\lambda = 1.5418$ ); (scanned angle from  $3^\circ$  to  $40^\circ$  with scanning speed of  $0.02^\circ$  per second). Mineral percentages were quantified from X-Ray Diffractogram using baseline fit method.

## SEDIMENTARY FACIES

The flood plain sequence at Bhimpura shows a trough having cross-bedded gravel and sand at the base followed by massive unstratified sandy-silty facies (0-1503 cm). The massive unstratified sandy-silty sediment is characterized based on grain size record (Folk 974) of the flood plain sequence, that is, fourteen aforesaid sieve fractions. The unstratified sandy-silty facies from a depth of 0-580 cm has calcrete in 420  $\mu\text{m}$  and 250  $\mu\text{m}$  sieve fractions.

Sediment facies from 0-580 cm depth were classified based on field as well as grain size data using cluster analysis technique. Four sediment facies that occur within 0 – 580 cm depth are defined as:

- (i) Massive unstratified very fine sand + fine sand ( $\text{Sm}_{\text{vfs+fs}}$ ) inferred from analyzing 16 samples consisting of 48% very fine sand, 42% fine sand and 10% silt
- (ii) Massive unstratified very Fine Sand + silt + fine sand ( $\text{Sm}_{\text{vfs+si+fs}}$ ) inferred from 22 samples having 61% very fine sand, 18% fine sand and 21% silt
- (iii) Massive unstratified very fine sand ( $\text{Sm}_{\text{vfs}}$ ), inferred from analyzing 30 samples comprising 73% of very fine sand 14% fine sand and 13% silt and
- (iv) Massive, unstratified silt + very fine sand ( $\text{Sm}_{\text{si+vfs}}$ ), derived from analyzing 7 samples.  $\text{Sm}_{\text{si+vfs}}$  facies have 59% very fine sand, 30% silt and 11% fine sand (Fig. 2c).

The lower part of the section is characterized by  $\text{Sm}_{\text{vfs+si+fs}}$  facies, which are uniformly developed from depth 580-433 cm. This is overlain by intercalation of  $\text{Sm}_{\text{vfs}}$  facies with facies of  $\text{Sm}_{\text{si+vfs}}$ ,  $\text{Sm}_{\text{vfs+si+fs}}$  and  $\text{Sm}_{\text{vfs+fs}}$  from 433-114 cm depth. Finally, the section is capped by a uniformly developed  $\text{Sm}_{\text{vfs}}$  facies from depth 114 cm to 0 cm. These changes in sediment characteristics can be correlated with significant changes in the intensity of the continental processes (fluvial and aeolian type).

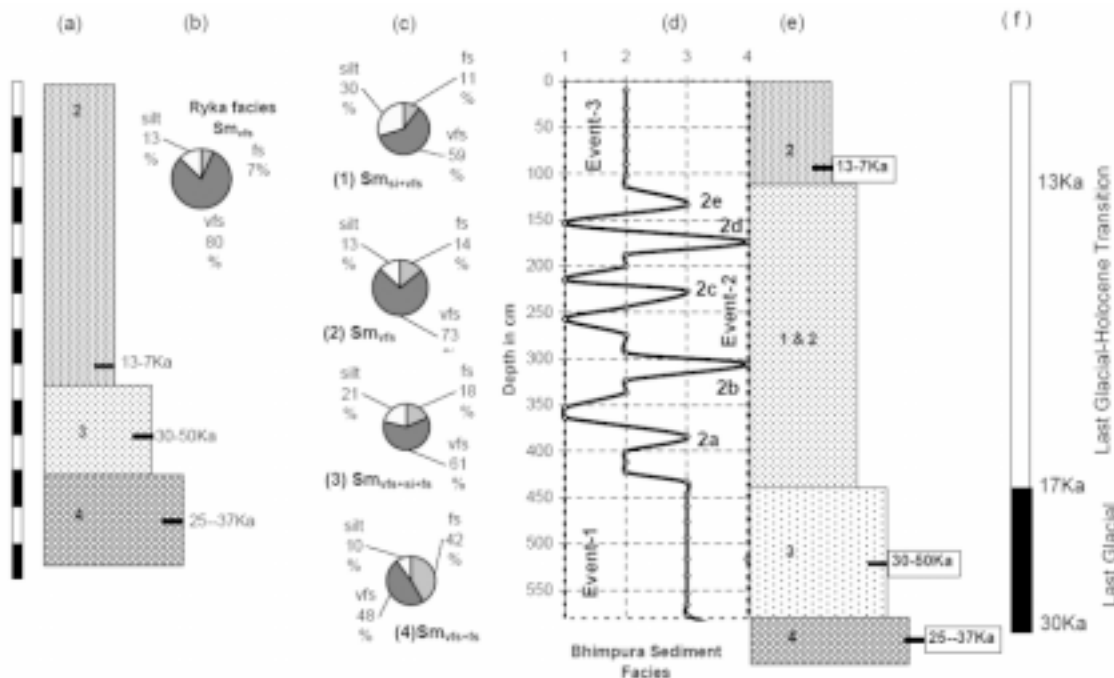


**Figure 2.** Details of litho facies from Bhimpura and Rayka. a) Litholog of Ryka section along with luminescence ages (Juyal et al. 2000); b) Sediment facies at Ryka section; c) Sediment facies at Bhimpura, namely: 1) Massive, unstratified silt + Very fine sand + silt ( $\text{Sm}_{\text{si+vfs}}$ ), 2) Massive unstratified very fine sand ( $\text{Sm}_{\text{vfs}}$ ), 3) Massive unstratified very Fine Sand + silt + fine sand ( $\text{Sm}_{\text{vfs+si+fs}}$ ) and 4) Massive unstratified very fine sand + fine sand facies ( $\text{Sm}_{\text{vfs+fs}}$ ). d) Change in facies at Bhimpura decoded using cluster analysis. X-axis represents sediment facies while Y-axis represents depth. Events and sub-events are separately marked. e) Litholog of Bhimpura section (0-580 cm). The number within litholog represents facies code, while the number in rectangle represent interpolated ages of individual sediment facies. f) Age model for Bhimpura section.

Grain size fractions sensitive to changes in process intensity and thereby climate, are identified using correlation analysis, across as well as within the facies clusters. This analysis suggests that 149  $\mu\text{m}$  grain size, a component of fine sand fraction and  $<25\mu\text{m}$ , the finest component of silt fraction are two allogenic representative proxies which correlate with floods and intense aeolian activity within flood plain. Increase in 149  $\mu\text{m}$  grain size fraction represents higher carrying capacity of rivers and therefore suggests wet climatic phase, whereas increase in  $<25\mu\text{m}$  grain size fraction represents weaker fluvial activity in a flood plain in addition to mobilization and accumulation of silt size particles by stronger aeolian activity which further suggest drier climatic phase.

Standard deviation within the 14-sieve size fraction is calculated for each sample to assess the spread in grain size. This characterizes the variability of grain size composition within a sediment package and is a proxy for the fluctuation in energy condition of the process responsible for deposition. Consequently, it is also sensitive to climate changes. Increase in standard deviation shows decrease in sorting and vice versa. The behavior of standard deviation with depth matches well with that of the representative grain size fractions considered above and hence further validates our choice. Fig. 3 shows the variation of facies cluster, 149  $\mu\text{m}$ ,  $<25\mu\text{m}$  grain size fractions and standard deviation with depth.

### MINERAL MAGNETIC PROPERTIES

Earlier studies on magnetic susceptibility from loess deposit in China suggest low frequency mass susceptibility  $\chi_{\text{LF}}$  which captures changes in a sequence showing high-grade pedogenesis whereas frequency dependent magnetic susceptibility  $\chi_{\text{FD}} (\%)$  records changes in low grade weathering [Heller et al. 1991; Guo et al. 2000]. In case of the present flood plain consisting of sediments deposited by monsoonal river system, the role of both allogenic (fluvial / aeolian) as well as authigenic processes (pedogenesis/ calcretization) can be discerned. The  $\chi_{\text{LF}}\text{bulk}$  and  $\chi_{\text{FD}}\text{bulk}$  record (Fig. 4) show inverse relationship. Increase in  $\chi_{\text{LF}}\text{bulk}$  indicates pedogenic horizon whereas increase in  $\chi_{\text{FD}}\text{bulk}$  indicates weaker pedogenesis along the section. Various pedogenic horizons distinguished in this deposit are based on magnetic susceptibility at different depths viz., 566-553 cm, 383-293 cm and 173-154 cm. This is further confirmed by the ferrimagnetic mineral percentage, which shows a positive correlation with  $\chi_{\text{LF}}\text{bulk}$  (Fig. 4).

### CARBONATE PERCENTAGE

Variation of carbonates along the section can be accessed both as percentage of carbonate and calcrete concentration as determined from  $<25\mu\text{m}$  using standard 1N HCL treatment using 420 $\mu\text{m}$  and 250 $\mu\text{m}$  sieve fractions respectively. Calcrete and carbonate percentage do not show significant correlation. The calcrete concentration shows positive relationship with 149 $\mu\text{m}$  and sediment facies, while the carbonate shows inverse relationship with  $<25\mu\text{m}$  and  $\chi_{\text{LF}}\text{bulk}$  (Fig. 4). Carbonate percentage from depth 553 cm to the top of the section increases from 35% to 57%, whereas calcrete percentage increases considerably at three depths, 306 cm, 446 cm and 516 with an average percentage increase lying between 18 and 21%.

### MINERALOGY

Percentages of seven minerals namely, quartz, feldspars, calcites, smectite, chlorite, illite, and hematite were quantified from 580 cm to 0 cm at about 45 cm interval. The variation in the mineralogical composition for three distinct facies at depths 580-433 cm, 433-411 cm and 411-0 cm (Fig. 5) has been observed. It is found that the percentage of quartz and feldspar decreases upward, whereas calcite percentage increases.

### AGE RELATIONSHIP

Interpretation of the paleoclimatic information from continental sediments at Bhimpura site requires development of a time scale. Records from Chinese loess plateau represent continental response to climate change. Two main techniques are used in age modeling on Chinese loess plateau viz., absolute age technique or correlation technique (Kohfeld 2001). To interpolate age for Bhimpura section, both these techniques, together with absolute luminescence age of Rayka type section in lower reaches of Mahi basin have been used.

Rayka section is located upstream about 12.5 km north within the lower reaches of Mahi valley. Earlier workers have laterally compared sediment facies within Mahi basin across various sections within lower reaches of Mahi basin highlighting lateral extension of facies (Pant & Chamyal 1990; Khadkikar et al. 1999; Malik et al. 1999). The sediment facies and luminescence dates along the Rayka section (Juyal et al. 2000) are also laterally co-relatable (Fig. 2).

The age model has been fine-tuned by comparing proxy record from Bhimpura with  $\delta^{18}\text{O}$  record of

Characterization of flood plain and climate change using multi-proxy records from the Mahi River Basin, Mainland Gujarat

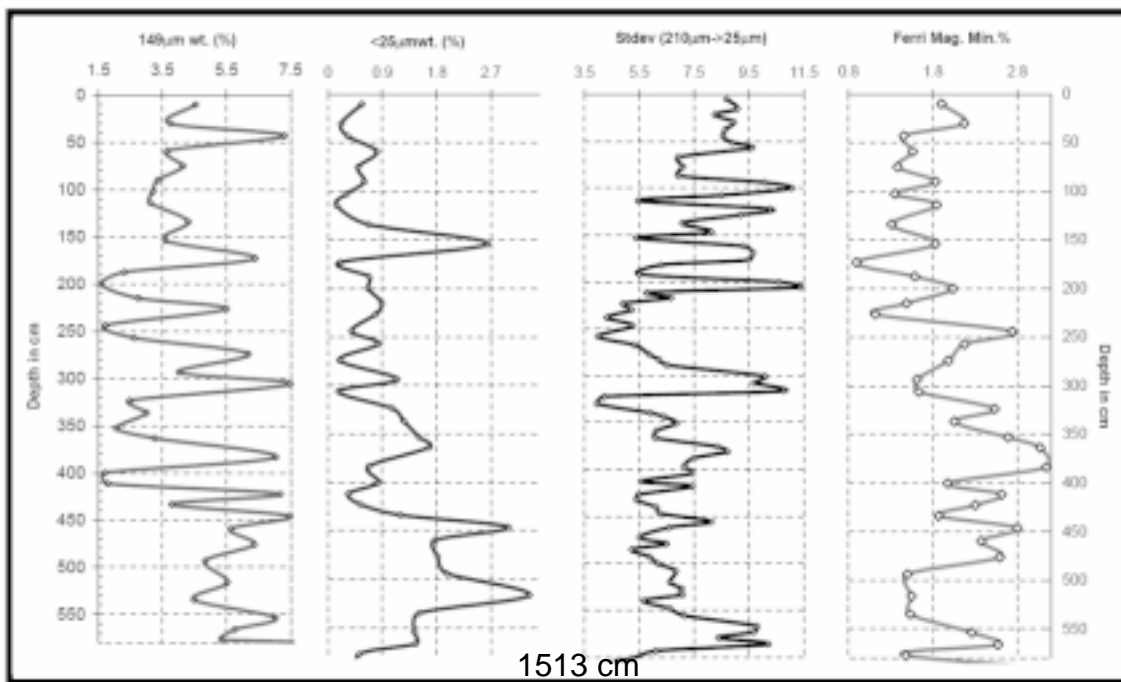


**Figure 3.** Climate sensitive allogenic proxy namely  $149\text{ }\mu\text{m}$  and  $<25\text{ }\mu\text{m}$  grain size fractions, Standard deviation and ferrimagnetic mineral percentage.

Note: In figure 3., All the parameters are from depth 0 to 580cm except Stdev which from depth 0 to 1513cm.

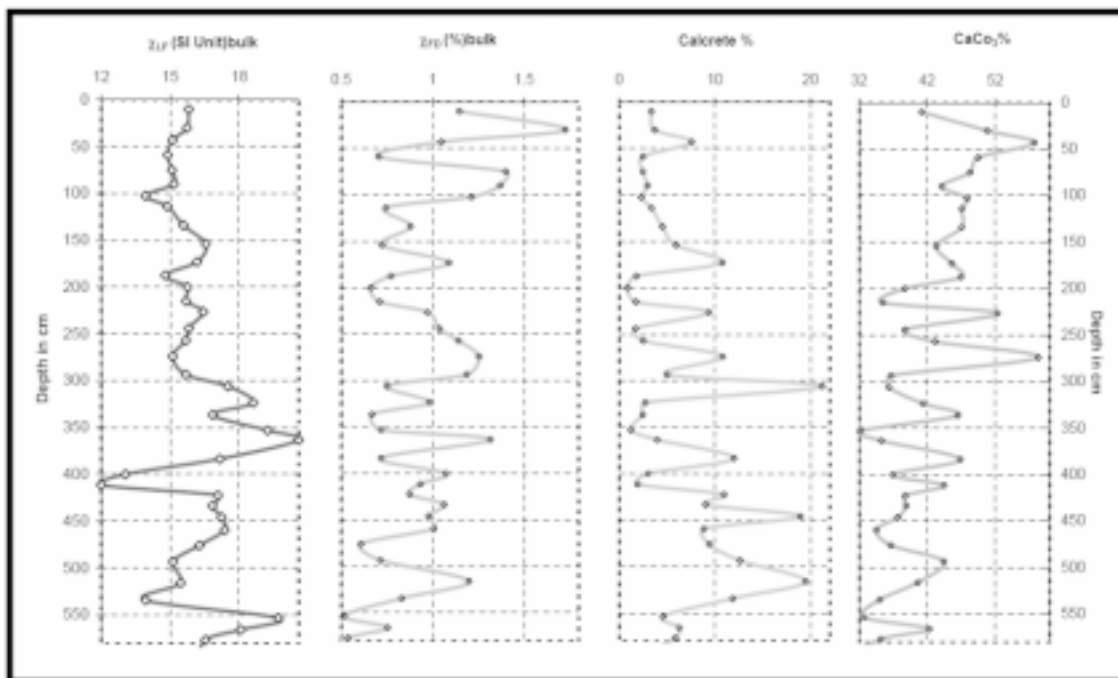


**Figure 4.** Climate sensitive allogenic and authigenic proxies namely magnetic susceptibility ( $\chi_{LF}$  bulk, and  $\chi_{FD}$  %bulk), calcrete percentage and carbonate percentage.

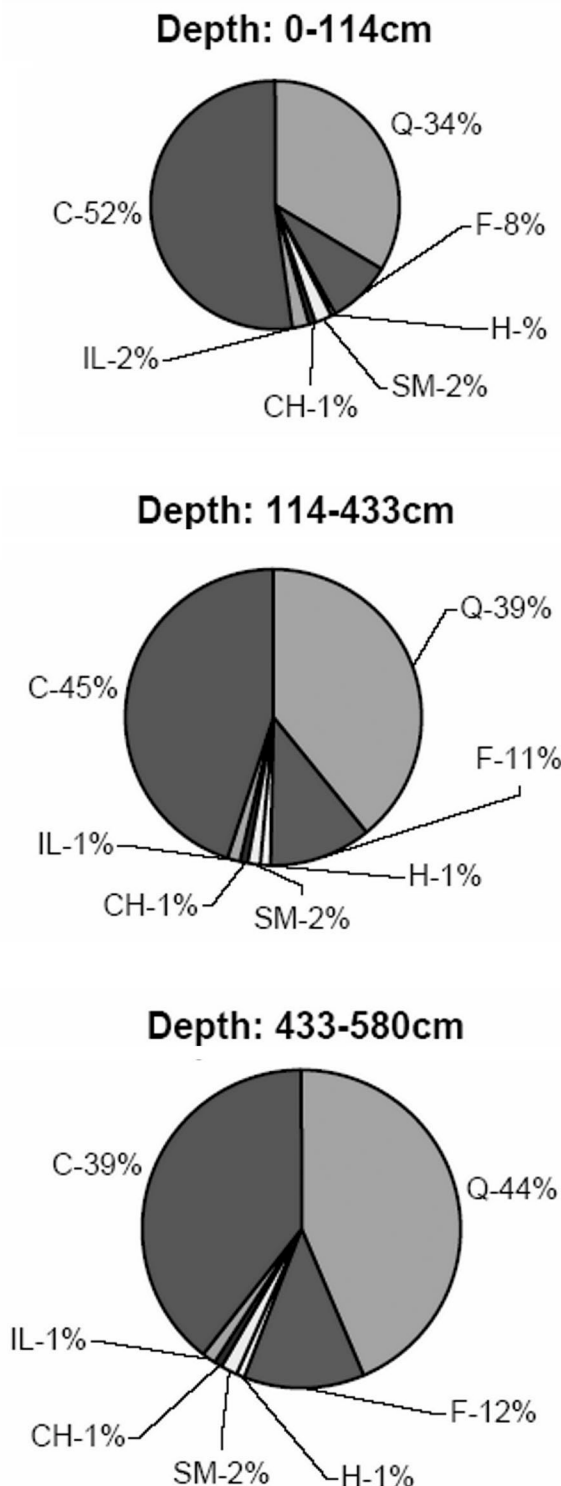


**Figure 5.** Bulk variation of minerals along depth 0-114 cm, 114-433 cm and 433 cm-580 cm.

Guliya ice core ( $35^{\circ}17'N$ ,  $81^{\circ}29'E$ ; 6200m a.s.l) and Qinghai-Tibetan Plateau (Thompson et al. 1997). The matching of flood plain sediment record is justified since the release of heat flux over the Qinghai -Tibetan Plateau drives the southwest Indian Monsoon (SwIM), which in turn causes intensity changes in the fluvial processes over the subcontinent (Sirocko et al. 1993; Overpeck et al. 1996; Thompson et al. 1997; Rangarajan & Sant 2000; Sant & Rangarajan 2002). Response of climate change at Guliya ice core was also recorded in Arabian Sea marine core 74KL (Rangarajan & Sant 2000). Also, the role of Indian Ocean in SwIM is well explained (Schulz et al. 1998). Therefore, the comparison of Bhimpura sediment record with Guliya ice core record would help us understand the interrelationship between continental ice core, continental flood plain sediments and Arabian Sea marine sediments, which are all tied together by the common global climatic system, SwIM.

Correlation of facies along Rayka section with Bhimpura litho facies gives three ages for three distinct facies units. The base of the section occurring at Bhimpura is marked by  $Sm_{vfs+fs}$  facies at 577-660 cm depth and is correlated with sandy-silty facies of Rayka occurring at 1350-1110 cm depth. Sandy silty facies form the late part of aggradation phase II and are dated as  $31 \pm 6$  ka (Juyal et al. 2000). This is the youngest pre-Holocene humid phase in Mahi and Sabarmati basin (Tandon et al. 1997; Juyal et al. 2000; Srivastava et al. 2001). This event is also correlated to oxygen isotope stage 3 after which the fluvial regime declined and aeolian regime began (Juyal et al 2003). The section under present study rests on the sediment deposited by the aforesaid event (Fig. 2).

The horizon with  $Sm_{vfs+si+fs}$  facies at depth 533 cm, immediately above  $Sm_{vfs+fs}$  facies shows pedogenic horizon (based on  $\chi_{LF}$  bulk record) and is comparable with red soil litho unit of Rayka section occurring between 840 cm and 1110 cm depth. This has been dated as  $40 \pm 10$  ka (Fig. 2). Because of the age reversal and larger error bar of date for red soil, the age of section at 580 cm has been considered as 30 ka.  $Sm_{vfs}$  that caps the Bhimpura section (114 cm to 0 cm) is correlated with aeolian sand unit of Rayka section (0-840 cm) that is dated to be about  $10 \pm 3$  ka (Fig. 2). Presence of microliths on the top surface of the Bhimpura mound is also observed. The luminescence dates on sand horizon at Langhnaj Dune (Sabarmati basin) that comprises of microliths were dated as  $11 \pm 3$  ka (base of horizon) and  $9 \pm 1$  ka (top of horizon) (Singhvi et al. 1982). Further, a maximum age for microliths at Langhnaj was estimated to be 10.5 ka (Wasson et al. 1983). Based on the Rayka dates and presence of microlith, the top of Bhimpura section is considered around 10ka.

The age interpolation thus obtained (Fig. 2d,e) is consistent with the luminescence dates within their error margin (Juyal et al. 2000). We consider interpolated luminescence dates for Bhimpura record and further fine tune the age by comparing various climatic events with  $\delta^{18}\text{O}$  record from Guliya ice core. We postulate that the change observed in sediment characteristics and other parameters along the depth profile, is the consequence of change in the intensity of the continental processes (fluvial / aeolian) during the period of deposition as a response to regional climatic change. Thus the Bhimpura sediments from depth 580–0 cm are found to capture climatic events that occur between late Glacial and Glacial-Holocene transition phase. The important climatic events observed from 30 ka to 10 ka are: Last Glacial Maxima, onset of climate change, Glacial-Holocene Transition phase, and Younger Dryas.

## CLIMATE CHANGE

Multi-proxy records for massive unstratified sandy-silty Bhimpura sediments are analysed to understand variability of each parameter along depth. Further, the age model is superimposed to characterize the age of events. The overall climate change within the SWIM system can be explained by comparing  $\delta^{18}\text{O}$  record from the Guliya ice core (Thompson et al. 1997) with the marine core 74KL [14° 19'16"N; 57° 20' 49"E; 3212m asl] (Sirocko et al. 1993). Based on multi-proxy record at Bhimpura, three major events and five sub-events can be discerned.

Event 1 is characterized from sediment at depth 580–433 cm, which shows development of uniform  $\text{Sm}_{\text{vfs+si+fs}}$  facies with relatively well-sorted sediment, suggesting a single process deposited these sediments. The representative alloogenetic proxy 149  $\mu\text{m}$  (proxy for fluvial process) shows decrease in percentage, whereas <25  $\mu\text{m}$  (proxy for aeolian process) shows significant increase. Ferrimagnetic mineral percentage also shows significant drop in percentage between 534 cm and 483 cm. Drop in percentage of higher density ferrimagnetic mineral suggests an influence of change in the process. This signature is also reflected in decrease in the  $\chi_{\text{LF}}$  bulk record as well as increase in the  $\chi_{\text{FD}}/(\%)$  bulk record. Percentage increase of calcrete and carbonate records at depths 516 and 493 cm suggest aridity enhancement.

The <25  $\mu\text{m}$  grain size fraction shows an overall increase from depth 580 cm onwards. Peaks at 516 and 446 cm suggest Last Glacial Maxima (LGM), after which it drops sharply. Studies on dunal deposits on the southern margin of Thar Desert (Mahi and Sabarmati basin) suggest active formation of dunes

around 26 ka with decline in the humid phase at Oxygen Isotope stage – 3 (OIS-3: 30ka) (Juyal et al. 2003). Thus, the sediment belonging to last Glacial phase and LGM has been characterized using the representative section at Bhimpura site.

Further, at Bhimpura, above 446 cm a consistent drop in the quantity of <25  $\mu\text{m}$  grain size fraction till 411 cm is observed. Similar signature is visible in other records such as sediment facies and degree of sediment sorting. This suggests the onset of a climate change from Last Glacial Phase to Holocene. A large number of dates of sediments at various sites in the Mahi- Sabarmati region define the chronology of LGM. However, we are unable to comment on the age for the onset of climate change due to lack of comparable records. Tentatively, onset of climate change from Last Glacial to Holocene can be placed between 26 ka and 17 ka.

The observation made by other workers in the Thar suggests that LGM record is missing from Thar sediments (Chawla et al. 1992; Kar et al. 2001; Juyal et al 2003). For instance, Wasson et al (1984) studied lake record from Didwana (27° 20'N; 74° 35'E) located along northeastern margin of Thar. They assigned 13 ka BP for the onset of significant clastic sedimentation that reflects change in hypersaline conditions prevailing with deposition of halite since Last Glacial. This has enabled Sant & Rangarajan (2002) to suggest a delayed response of LGM at Didwana by 5.8 kyrs.

The onset of climate change was recorded over loess plateau where tropical Pacific had played an initial and vital role in triggering a climate change at around 21.5 ka B.P. This was followed by initiation of warming over Tibetan plateau (as recorded in Guliya ice core) at 18.8 ka BP, as a consequence of the green house gases feedback cycle. The warming at Tibetan Plateau led to a large scale melting of ice sheets. This large-scale influx of water into the Arabian sea affected the marine core 74KL. Based on  $\delta^{18}\text{O}$ , a temperature proxy and total rare earth elements, a proxy for melt water influx, a delayed response at 17.5 ka in this marine core is inferred (Sant & Rangarajan 2002). Consequently, we propose that the flood plains have enough potential to capture large-scale changes in climate in terms of decrease in aeolian phases and onset of flooding events. The estimated age for onset of climate change could be further narrowed down to anywhere between 18 ka and 17 ka.

Event 2 is characterized by intercalation of  $\text{Sm}_{\text{vfs+fs}}$  facies and  $\text{Sm}_{\text{vfs+si+fs}}$  facies (coarser component) with  $\text{Sm}_{\text{vfs}}$  facies and  $\text{Sm}_{\text{si+vfs}}$  facies (finer component) from 422 cm to 114 cm depth. Event 2 consists of a group of five sub-events namely: Event-2a at 383 cm; Event-

2b at 306 cm; Event-2c at 226 cm; Event-2d at 173 cm and Event-2e at 134 cm. The sub-events 2a to 2e are characterized by  $Sm_{vfs+fs}$  and  $Sm_{vfs+si+fs}$  facies and increase in sorting. Further, the representative allogenic proxy  $149\ \mu m$  (proxy for fluvial process) shows significant increase in percentage. Between each sub-event within Event 2, intercalation by  $Sm_{vfs}$  and  $Sm_{si+vfs}$  facies is found. These sediment facies show sharp decrease in sorting and a quantitative decrease in  $149\ \mu m$  grain size fraction. It is observed that an increase in  $<25\ \mu m$  grain size fraction along these units with a significant increase at 363 cm depth between event 2a and 2b. This signature is also reflected in increase in  $\chi_{LF}$  bulk record as well as decrease in  $\chi_{FD}(\%)$  bulk record. Ferrimagnetic mineral percentage also shows significant drop during each sub-event except at sub-event-2a. Percentages of calcrete record suggest increase along sub-events except along event 2e, whereas percentage of carbonates increase at sub-events 2a, 2c, 2d and 2e and decrease at sub-event 2b. These five sub-events thus represent flooding events / wet phase (strong monsoon), whereas intercalated sediments ( $Sm_{vfs}$  facies and  $Sm_{si+vfs}$  facies) within two events show weak fluvial events supplemented with aeolian activity (weak monsoon). These rapid fluctuations over the flood plain represent a transition phase of climate from Last Glacial to Holocene.

Climatic processes affecting the above events can be explained as follows. During the dry phase (weak monsoon), the winds pick up available fine silt size grains from the flood plain and redistribute them over the region. On the other hand, during wet phase (strong monsoon) the torrential rains lead to catastrophic flash floods within shallow existing rivers that influence the denudation process. Channel avulsion, migration and incision over newly developed surface, composed of fluvio-aeolian deposit, would thus become a common phenomena. The fluctuation of climate during this transition will lead to overall building up of alluvial plain (aggradation) and be responsible for developing various fluvial landforms.

Event 3 is represented from depth 114 cm upwards. The anomalous uniformity ( $Sm_{vfs}$  facies) and sorting of the sediment during Event 3 show significant role of a single process suggesting an increase in aeolian activity. A similar feature is observed along other sections within the lower reaches of Mahi river basin (Khadkikar et al. 1999, Juyal et al. 2000). The luminescence age for last aeolian phase within Mahi river basin is dated to  $10 \pm 3$  ka (Juyal et al. 2000). Chronologically, this anomaly may represent signature of Younger Dryas (YD). The regional record

of YD is not well understood. However, the records from the region influenced by SwIM system suggest YD extends from 13.2 to 10.8 ka in Guliya ice core (Thompson et al. 1997); 11.55 to 10.88 ka in 74KL (Sirocko et al. 1993); 12.95 to 11.45 ka in 93KL (Schulz et al. 1998) and 12.1 to 10.7 Ka in Vostok ice core (Jouzel et al. 1987).

The sensitive allogenic proxy ( $149\ \mu m$  grain size fraction), ferrimagnetic percentage and  $\chi_{FD}(\%)$  bulk record also suggest a wet phase capping the 78 cm aeolian sediment representing YD. This event signals the onset of Holocene and termination of Last Glacial-Holocene transition.

It can be concluded that the massive unstratified sandy-silty sediments from flood plains in western India have enough potential for understanding the response to climate change that occurred from 30 ka to the onset of Holocene. Change in sediment facies, and climate sensitive proxies of  $149\ \mu m$  and  $<25\ \mu m$  grain size fractions, ferrimagnetic percentage (bulk), and magnetic susceptibility of the bulk sample as well as carbonate percentage and mineralogy deduced from  $<25\ \mu m$  grain size fraction capture both allogenic and authigenic processes. The Mahi river basin thus captures significant signatures of late stage of Last Glacial phase during which  $<25\ \mu m$  grain size fraction shows significant increase. Beginning of the rapid sub events- 2a to 2e marks the onset of climate change. During this part of climate transition, oscillation of five strong and weak monsoon periods has been identified. This is followed by strong aridity indicating YD from the signatures obtained at a depth of 114 cm and between 43 and 30 cm. The upper-most part of the section represents wet phase as shown by sensitive allogenic proxies that followed the YD. This event marks the onset of Holocene.

We conclude with a final observation that microliths on the top of mound suggest human cultural activities flourished soon after the onset of interglacial (Holocene) marked by a wet phase in the study area.

## ACKNOWLEDGEMENTS

This work was supported in part by a grant from the Department of Science and Technology, India. DAS would like to thank the Nonlinear Studies Group, Indian Institute of Science, Bangalore for support. GR was also supported by the Homi Bhabha Fellowship. The authors would like to thank Prof. S. N. Rajaguru, Prof. V. H. Sonawane, Dr. V. Purnachandra Rao, Dr. Aniruddha S. Khadkikar and Dr. Shashikant Acharya for useful discussions.

## REFERENCES

Allchin B. & Goudie, A. 1971. Dunes, aridity and early man in Gujarat, western India, *Man*, 6, 248-265.

Allchin, B., Goudie, A. & Hegde, K., 1978. The Prehistory and Palaeogeography of the Great Indian desert, Academic Press, London, 370 p..

Castellrott S. & Driessche J. V., 2003. How plausible are high frequency sediment supply-driven cycles in the stratigraphic record?, *Sediment. Geol.*, 157, 3-13.

Chawla, S., Dhir, R.P. & Singhvi, A.K., 1992 Thermoluminescence chronology of sand profile in the Thar desert and their implications, *Quat. Sci. Rev.*, 11, 25-32.

Folk R.L. 1974. Petrology of sedimentary rocks. Hemphill Publishing Co. Drawer M. University station austin, Texas 78712, 182.

Guo, Z., Biscaye, P., Wei, L., Chen. X., Peng, S., Liu, T. 2000. Summer monsoon variation over the last 1.2 Ma from the weathering of loess-soil sequence in China, *Geophys. Res. Lett.*, 27, 1751-1754.

Heller, F., Liu, H.Y., Liu, T.S. & Xu, T. 1991. Magnetic suseptibility of loess in China. *Earth Planet. Sci. Lett.*, 103, 301-310.

Juyal, N., Rachna Raj, Maurya, D.M., Chamyal, L.S. & Singhvi, A.K., 2000. Chronology of late Pleistocene environmental changes in the lower Mahi basin, western India, *J. Quat. Sci.*, 15, 501-508.

Juyal, N., Kar, A., Rajaguru S.N. & Singhvi, A.K. 2003. Luminescene chronology of aeolian deposition during the late quaternary on the southern margin of Thar Desert, India. *Quat. Inter.*, 104, 87-98.

Jouzel, J., Lorius, C., Petit, J.R., Genthon, C., Barkov, N.I., Kotlyakov V.M. & Petrov, V.M., 1987. Vostok ice core: A continuous isotope temperature record over the last climate cycle 160, 000 years, *Nature*, 329, 403-408.

Kar, A., Singhvi, A.K., Rajaguru, S.N., Juyal, N., Thomas, J.V. Banerjee, D. & Dhir, R.P., 2001. Reconstruction of Late Quaternary environment of the Lower Luni Plain, Thar Desert, India *J. Quat. Sci.*, 36, 217-229.

Khadkikar, A.S., Mathew, G., Malik, J.N., Gundu Rao, T.K., Chowgaonkar M.P. & Merh, S.S., 1999. The influence of the south-west Indian monsoon on continental depositional over past 130 kyr, Gujarat, western India, *Terra Nova*, 11, 273-277.

Knox, J.C., 2000. Sensitivity of modern floods to climate change, *Quat. Sci. Rev.*, 19, 439-457.

Kohfeld, K.E., 2001. Late Quaternary aeolian deposition on the Chinese Loess Plateau. In MPI-BGC Tech Rep.3 eds. K. E. Kohfeld & S. P.Harrison, 23-26.

Macklin, M.G. & Lewin, J., 2003. River sediment, great floods and centennial-scale Holocene climate change, *J. Quat. Sci.*, 18, 101-105.

Malik, J.N., Khadkikar A.S. & Merh, S.S., 1999. Allogenic control on late Quaternary continental sedimentation in the Mahi River basin, western India, *J. Geol. Soc. India*, 53, 299-314,

Merh, S.S. & Chamayal, L.S., 1997. The Quaternary geology of the Gujarat Alluvial Plain, *Proc. Indian Nat. Sci. Acad.*, 63A, 1-98.

Overpeck, J., Anderson, D., Trumbore S. & Prell, W., 1996. The southwest Indian monsoon over last 18,000 years, *Clim. Dyn.*, 12, 213-225.

Pant R.K. & Chamyal, L.S., 1990. Quaternary sediment pattern and terrain evolution in the Mahi river basin, Gujarat, India, *Proc. Indian Nat. Sci. Acad.*, 56, 501-511,

Rangarajan, G. & Sant, D.A., 2000. Paleoclimatic data from 74KL and Guliya cores: New insight, *Geophys. Res. Lett.*, 27, 787-790.

Sant, D.A. & Rangarajan, G., 2002. Onset of climate at Last Glacial-Holocene transition: Role of the tropical Pacific, *Curr. Sci.*, 83, 1398-1402.

Schulz, H., von Rad, U. & Erlenkeuser, H., 1998. Correaltion between Arabian Sea and Greenland climate oscillations of the past 111,000 years, *Nature*, 393, 54-57.

Shukla, J., 1975. Effect of Arabian sea-surface temperature anomaly on Indian summer monsoon: a numerical experiment with GFDL model, *J. Atmos. Sci.*, 32, 503-511.

Shukla, J. & Mishra B.M., 1977. Relationship between sea surface temperature and wind speed over the central Arabian Sea, and monsoon rainfall over India, *Mon. Weath. Rev.*, 105, 98-102.

Singhvi, A.K., Sharma, Y.P. & Agrawal, D.P., 1982. Thermoluminescence dating of sand dune in Rajasthan, *Nature*, 295, 313-315.

Sirocko, F., Sarnthein, M., Erlenkeuser, H., Lange, H., Arnold, M. & Duplessy, J.C., 1993. Century-scale events in monsoonal climate over past 24000 years, *Nature*, 354, 322-324.

Sridhar, V., Chamyal, L.S. & Merh, S.S., 1994. North Gujarat rivers: Remnants of a super fluvial system, *J. Geol. Soc. India*, 44, 427-434.

Srivastava, P., Juyal, N., Singhvi, A.K., Wasson, R.J. & Bateman, M.D., 2001. Luminescence chronology of river adjustment and incision of Quaternary sediment in the alluvial plain of the Sabarmati River, north Gujarat, India, *Geomorphology*, 36, 217-229.

Subbarao, B., 1952. Archaeological explorations in Mahi valley, J. M.S. Univ., Baroda, 1, 33-74.

Tandon, S.K, Sareen, B.K., Someshwar Rao, M. & Singhvi, A.K., 1997. Aggradation history and luminescence chronology of late quaternary semi-arid sequence of the Sabarmati basin, Gujarat, western India, *Palaeogeog. Palaeoclimat. Palaeoecol.*, 128, 339-357.

Thompson, L.G., Yao, T., Davis, M.E., Henderson, K.A., Thompson, E.M., Lin, P.N., Beer, J., Synal, H.A., Cole-Dai, J. & Bolzan, J.F., 1997. Tropical climate instability: The last Glacial cycle from a Qinghai-Tibetan ice core, *Science* 276, 1757-1825.

Wasson, R.J., Rajaguru, S.N., Mishra, V.N., Agrawal, D.P., Singh, R.P., Singhvi, A.K. & KameswarRao, K., 1983. Geomorphology, late Quaternary stratigraphy and palaeoclimatology of the Thar dunefield, *Zeit. Geomorph.*, 45, 117-151.

Xiao J., Porter, S.C., An, Z., Kumai, H. & Yoshikawa, S. 1995. Grain size of quartz as an indicator of wintermonsoon strength on the loess plateau of central China during the last 130,000 yr, *Quat. Res.*, 43, 22-29.

Zeuner, E. 1950. Stone age and Pleistocene chronology in Gujarat, Deccan College Monogram Series 6, 46 p.